t-CHANNEL UNITARITY CONSTRUCTION OF SMALL-x KERNELS*

C. CORIANÒ[a,b] AND A.R. WHITE[a]

[a]High Energy Physics Division
Argonne National Laboratory
9700 South Cass, Il 60439, USA
[b]Institute for Fundamental Theory
Department of Physics, University of Florida
Gainesville, FL 32611, USA

(Received November 3, 1995)

We present the BFKL equation as a reggeon Bethe–Salpeter equation and discuss the use of reggeon diagrams to obtain 2-2 and 2-4 reggeon interactions at $O(g^4)$. We then outline the dispersion theory basis of multiparticle j-plane analysis and describe how a gauge theory can be studied by combining Ward identity constraints with the group structure of reggeon interactions. The derivation of gluon reggeization, the $O(g^2)$ BFKL kernel, and $O(g^4)$ corrections, is described within this formalism. We give an explicit expression for the $O(g^4)$ forward "parton" kernel in terms of logarithms and evaluate the eigenvalues. A separately infra-red finite component with a holomorphically factorizable spectrum is shown to be present and conjectured to be a new leading-order partial-wave amplitude. A comparison is made with Kirschner's discussion of $O(g^4)$ contributions from the multi-Regge effective action.

PACS numbers: 11.55.Jy, 12.38.Lg

1. Introduction

In the leading-log approximation, the small-x behavior of parton distributions in QCD is derived from the BFKL evolution equation [1]. It is well-known that the BFKL kernel is (and was derived as) a 2-2 reggeon interaction — with the reggeon being a reggeized gluon. For general t $(= -q^2)$

* Presented by Alan R. White at the XXXV Cracow School of Theoretical Physics, Zakopane, Poland, June 4–14, 1995.

the BFKL equation becomes a reggeon Bethe–Salpeter equation as illustrated in Fig. 1.1

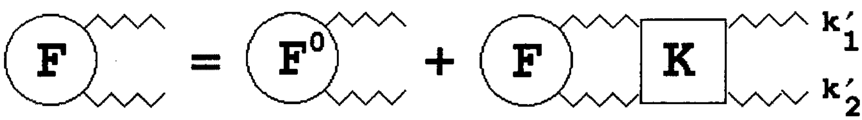

Fig. 1.1. Reggeon Bethe–Salpeter equation.

where $F \equiv F(\omega, k_1, k_2)$ is (the Fourier transform of) a two-reggeon amplitude which becomes a parton distribution when $k_1 + k_2 = 0$. The two-reggeon intermediate state integration is

$$\equiv \int \frac{d^2k_1}{k_1^2}\frac{d^2k_2}{k_2^2}\frac{\delta^2(k_1' + k_2' - k_1 - k_2)}{\omega - \Delta(k_1^2) - \Delta(k_2^2)}, \tag{1.1}$$

where $\Gamma_2 = [\omega - \Delta(k_1^2) - \Delta(k_2^2)]^{-1}$ is a two-reggeon propagator and

$$\Delta(q^2) = Ng^2 J_1(q^2) = \frac{Ng^2}{16\pi^3}\int \frac{d^2k}{k^2(k-q)^2}\,. \tag{1.2}$$

The 2-2 reggeon interaction $K(k_1, k_2, k_1', k_1')$ is given by

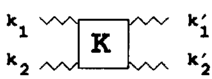

$$= Ng^2\left(\frac{k_1^2 k_2'^{\,2} \;+\; k_2^2 k_1'^{\,2}}{(k_1 - k_1')^2} - (k_1 + k_2)^2\right). \tag{1.3}$$

The familiar BFKL kernel is

$$\begin{aligned} K_{\mathrm{BFKL}}(k_1, k_2, k_1', k_1') = {} & K(k_1, k_2, k_1', k_1') \\ & - \Delta(k_1^2)\delta^2(k_1 - k_1') - \Delta(k_2^2)\delta^2(k_2 - k_2')\,. \end{aligned} \tag{1.4}$$

Generally reggeon interactions have been studied by s-channel unitarity calculations [1–5]. For example, calculation of the BFKL kernel can be represented schematically as in Fig. 1.2

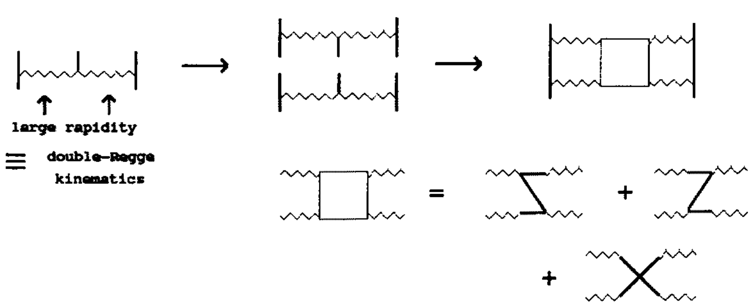

Fig. 1.2. Calculation of the BFKL Kernel via s-channel unitarity.

Alternatively we can "sew" reggeon amplitudes together via t-channel unitarity. The derivation of the BFKL kernel in this manner will be a core part of these lectures. It is illustrated schematically in Fig. 1.3.

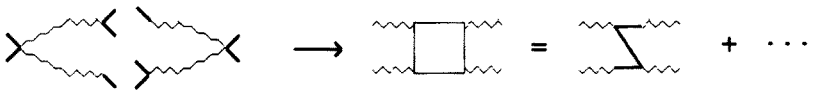

Fig. 1.3. Calculation of the BFKL Kernel via t-channel unitarity.

The "sewing" of Fig. 1.3 is well-defined if it is done in the j-plane (where $j = 1 + \omega$) by treating the particles appearing in the intermediate states also as reggeons [6, 7]. The analytic continuation of multiparticle unitarity equations in the j-plane is a powerful formalism [8, 9], essentially because of the underlying exploitation of multiparticle dispersion theory [10, 11] involved. We will briefly describe the full formalism later. First we observe that a simple (but "too naive") way to sew reggeon amplitudes together with reggeons acting as particles is to use reggeon diagrams directly.

1.1. Reggeon diagrams

t-channel unitarity is satisfied at the level of reggeon unitarity (see the later discussion) if we construct a set of reggeon diagrams as follows [12]. We introduce a triple regge vertex

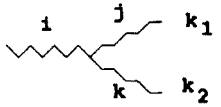

$$\sim g\, c_{ijk} \sqrt{\alpha'}\ [\omega - \alpha' k_1^2 - \alpha' k_2^2], \qquad (1.5)$$

where g is the gauge coupling, c_{ijk} is a structure constant color factor, and $[\ldots]$ is a "nonsense zero". We introduce propagators

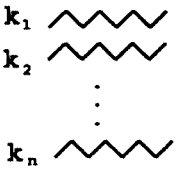

$$\equiv \prod_n = \Pi_{i=1}^n \left(\frac{1}{\alpha' k_i^2}\right) \frac{1}{\omega - \sum_{i=1}^n \alpha' k_i^2}. \qquad (1.6)$$

We then combine vertices and propagators by integrating over transverse momenta — with momentum conservation imposed. (A subtlety is that we actually have to construct "cut" reggeon diagrams for the imaginary part of amplitudes, but we will not elaborate on this).

The nonsense zeroes cancel many reggeon singularities leaving only *particle singularities generating arbitrarily high-order reggeon interactions.* The

outcome is a very simple formalism [12] for generating reggeon interactions. The interactions are automatically obtained in terms of *transverse momentum diagrams* which we introduce via the vertices and phase-space integrations illustrated in Fig. 1.4.

Fig. 1.4. (a)Vertices and (b) intermediate states in transverse momentum.

The rules for writing amplitudes corresponding to the diagrams are the following

- For each vertex illustrated in Fig. 1.4(a) we write a factor

$$16\pi^3\delta^2(\sum k_i - \sum k_i')(\sum k_i)^2$$

- For each intermediate state illustrated in Fig. 1.4(b) we write a factor

$$(16\pi^3)^{-n}\int \frac{d^2k_1\ldots d^2k_n}{k_1^2\ldots k_n^2}$$

The reggeization, of the gluon, is illustrated in Fig. 1.5

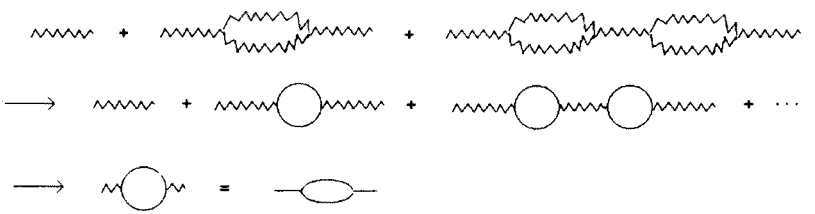

Fig. 1.5. Reggeization of the gluon from reggeon diagrams.

The origin of the BFKL kernel is illustrated in Fig. 1.6

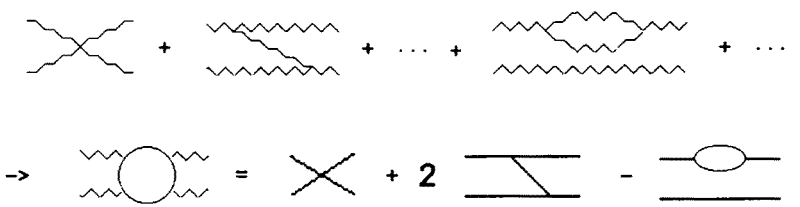

Fig. 1.6. The BFKL kernel from reggeon diagrams.

and the transverse momentum diagrams derived as $O(g^4)$ interactions in [12] are shown in Fig. 1.7.

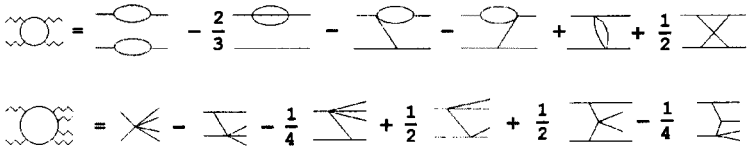

Fig. 1.7. $O(g^4)$ reggeon interactions.

In all of the above cases it can be shown [12] that if reggeon diagrams are used to generate the possible transverse momentum diagrams then, *in color zero channels, gauge invariance determines the relative coefficients uniquely.* Gauge invariance is imposed by requiring that

- all infra-red divergences cancel,
- reggeon interactions vanish when any transverse momentum goes to zero.

The cancellation of infra-red divergences is, essentially, an obvious consequence of gauge invariance. As we now elaborate, imposing the vanishing of reggeon amplitudes at zero transverse momentum is directly equivalent to imposing the defining Ward identities of the theory [13].

1.2. Gauge invariance and reggeon Ward identities

A reggeon amplitude is defined via a multi-Regge limit in which, say, $s_i \to \infty$ $i = 1, \ldots, 4$. Schematically we can write

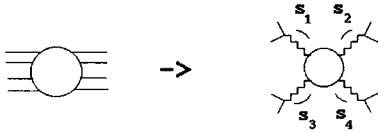

$$\equiv \Pi_{i=1}^{4} s_i^{\alpha_i} A_{\alpha_1,\alpha_2,\alpha_3,\alpha_4} . \qquad (1.7)$$

We can always find a Lorentz frame in which the limit $s_1 \to \infty$ is defined by $p_+ \to \infty, k \to k_\perp$ where p and k are as labelled in Fig. 1.8.

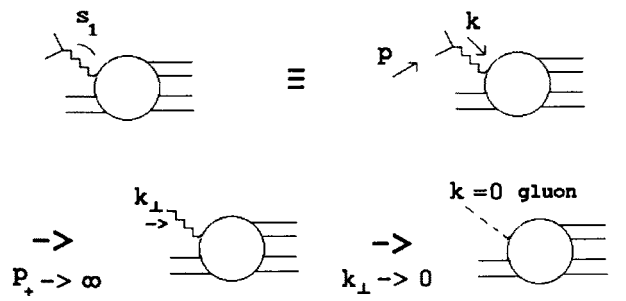

Fig. 1.8. Reduction of a reggeon amplitude to a gluon amplitude.

The further limit $k_\perp \to 0$ is then equivalent to setting $k = 0$. Reggeization implies the reggeon amplitude must give the $k = 0$ gluon amplitude. Therefore, we obtain the zero momentum limit of an amplitude which satisfies a Ward identity [13]

$$k_\mu \langle A_\mu(k) \ldots \rangle = 0 , \tag{1.8}$$

where $\langle A_\mu(k) \ldots \rangle$ is the amplitude involving a gluon with momentum k_μ. Differentiating

$$\langle A_\mu \ldots \rangle + \frac{\partial \langle A_\nu \ldots \rangle}{\partial k_\mu} k_\nu = 0$$

$$\Rightarrow \langle A_\mu \ldots \rangle \underset{(k_\mu \to 0)}{\longrightarrow} 0 \quad \text{if} \quad \frac{\partial \langle A_\nu \ldots \rangle}{\partial k_\mu} \not\to \infty . \tag{1.9}$$

If there are no internal infra-red divergences occurring explicitly at zero transverse momentum (as will be the case in the absence of massless fermions [14]), then this identity requires the amplitude to vanish. Clearly the same argument can be applied to each of the reggeons in (1.7).

1.3. Questions

A number of closely related questions arise from the reggeon diagram construction of reggeon interaction kernels. We can list some of the more obvious as follows.

1. The kernels are *scale-invariant in transverse momentum* — what is the significance of this "approximation"?
2. How is a scale(s) to be added?
   a) $g^2/4\pi \to \alpha_s(Q^2/\mu^2)$?
   b) A $k_\perp$ cut-off?
   c) An "average" rapidity $\langle \eta \rangle$ as a normalization [15]? It is generally anticipated that a full next-to-leading order calculation [3] will provide an answer to this question.
3. Why are there only transverse momentum integrals representing t-channel states?
4. What is the significance of properties related to conformal invariance?

In the following we will briefly describe a more fundamental derivation of $O(g^4)$ reggeon interactions directly from t-channel unitarity [16]. This formalism provides a solid basis within which to ask these questions and, at least partly, answer them. A major outcome will be the suggestion that *scale-invariant contributions that are well-defined by unitarity are necessarily conformally invariant.*

2. Multiparticle j-plane analysis

To introduce language, we first recall the simplest elements of Regge theory for elastic scattering amplitudes. The partial-wave expansion is

$$A(z,t) = \sum_{j=0}^{\infty}(2j+1)a_j(t)P_j(z)\,, \tag{2.1}$$

where

$$a_j(t) = \frac{1}{2}\int_{-1}^{+1} dz A(z,t)P_j(z)\,. \tag{2.2}$$

Using the dispersion relation

$$A(z,t) = \frac{1}{2\pi}\int_{I^R+I^L}\frac{dz'}{(z'-z)}\Delta(z',t)\,, \tag{2.3}$$

we obtain

$$a_j(t) = \frac{1}{4\pi}\int_{I^R+I^L} dz'\Delta(z',t)\int_{-1}^{+1}\frac{dz}{(z'-z)}P_j(z)\,, \tag{2.4}$$

giving "signatured" continuations from even and odd j

$$a_j^{\pm}(t) = \frac{1}{2\pi}\int_{I^R} dz' Q_j(z')\Delta(z',t) \pm (-1)^j\frac{1}{2\pi}\int_{I^L} dz' Q_j(-z')\Delta(z',t)\,. \tag{2.5}$$

The asymptotic behavior of A(z,t) can be studied via the Sommerfeld–Watson transform

$$A(z,t) = \sum_{\pm}\int dj\frac{(2j+1)}{4\sin\pi j}a_j^{\pm}(t)\Big(P_j(z)\pm P_j(-z)\Big) \tag{2.6}$$

and a Regge pole in $a_j^{\pm}(t)$ at $j=\alpha(t)$ gives

$$A(z,t)) \sim z^{\alpha(t)}\,. \tag{2.7}$$

The simplest example of "j-plane unitarity" is elastic unitarity.

$$a_j^{\tau} - a_j^{\tau *} = i\rho(t)a_j^{\tau}a_j^{\tau *} \qquad \tau = \pm\,. \tag{2.8}$$

This equation is inconsistent with a fixed pole in the j-plane. But apparently

$$Q_j(z) \underset{j\to -1}{\longrightarrow} \Gamma(j+1) \sim \frac{1}{j+1} \quad \Rightarrow \quad a_j^{\pm}(t) \underset{j\to -1}{\sim} \frac{1}{j+1} \tag{2.9}$$

and so there is a "nonsense" pole at $j = n_1 + n_2 - 1$ where, in this case, $n_1 = n_2 = 0$. In a gauge theory $n_1 = n_2 = 1$ is possible and so there is a "nonsense fixed-pole" at $j = 1$. The conflict with unitarity is resolved by the fixed pole mixing with the elementary gluon and producing Reggeization.

To analyse multiparticle unitarity in the j-plane, we need to generalize all of the elastic scattering formalism. We require

- Multiparticle, *many-variable*, dispersion relations.
  The analyticity properties of multiparticle amplitudes are very complicated but (20 years ago) it was shown [11, 10, 9] that, in multi-Regge asymptotic regions, the necessary dispersion relations hold. This is sufficient to obtain analytically continued partial-wave amplitudes [9]. Spectral components of the (asymptotic) dispersion relations are labeled by *hexagraphs*. These are tree graphs having the form illustrated in Fig. 2.1.

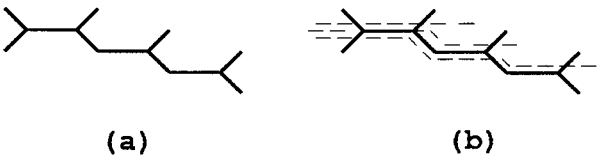

Fig. 2.1. (a) A hexagraph for the six-particle amplitude (b) cuts through the hexagraph.

Possible cuts through a hexagraph, as illustrated, give the multiple discontinuities of the spectral component that the graph represents.

- Continuations to complex *angular momenta and helicities.*
  For each hexagraph component, distinct continuations are possible and the hexagraph notation also indicates this. For example, introducing angular momenta and helicities corresponding to the elements of the hexagraph as in Fig. 2.2, a continuation can be made to complex j_1, n_2, and n_3 with $j_2 - n_2$ and $j_3 - n_3$ (which are coupled in the hexagraph) held fixed at integer values.

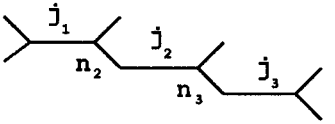

Fig. 2.2. Angular momenta and helicities associated with a hexagraph.

The complete set of hexagraph j- and n-plane continuations are sufficient [9] to write Sommerfeld-Watson transforms and obtain multi-Regge asymptotic behavior. These continuations are also sufficient to obtain the t-channel unitarity contributions of multi-Regge pole states that we discuss below. We shall find that *reggeon singularities are generated as Regge cuts* and that *particle singularities give reggeon interactions.*

Our ultimate aim is to construct "Yang–Mills reggeon theories" by using j-plane unitarity directly. We can bypass momentum-space calculations completely by using the following elements.

[**A**] Gauge invariance is input via the Ward identity constraint — that reggeon interactions vanish at zero transverse momentum.
[**B**] The "nonsense" zero/pole structure required by general analyticity properties is imposed, in addition to Ward Identity zeroes.
[**C**] The group structure is input via the triple reggeon vertex.
[**D**] t-channel unitarity is used to determine both j-plane Regge cut discontinuities and particle threshold discontinuities due to "nonsense" states.
[**E**] The j-plane and t-plane discontinuity formulae are expanded simultaneously around $j = 1$ and in powers of g^2.

2.1. Reggeon unitarity

We first go through a 30 year old [8, 9] manipulation of t-channel unitarity which, a-priori, is independent of gauge invariance. Consider the four-particle intermediate state as illustrated in Fig. 2.3.

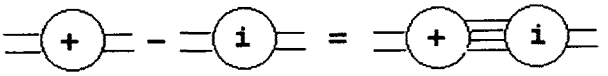

Fig. 2.3. The four-particle intermediate state.

The i denotes an amplitude evaluated on the unphysical side of the four-particle branch-cut. (We will avoid discussing subtleties associated with the definition of i amplitudes, in particular the specification of the additional boundary-values involved.) We use multiparticle partial-wave amplitudes corresponding to the "coupling scheme" illustrated in Fig. 2.4.

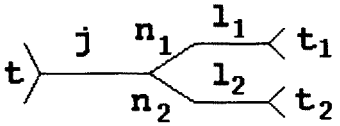

Fig. 2.4. Partial-wave coupling scheme for the 2-4 production amplitude.

$l_1(l_2)$ and $n_1(-n_2)$ are respectively the angular momentum and helicity (in the overall center of mass) of the two-particle state with invariant energy $t_1(t_2)$.

The partial-wave projection of Fig. 2.3 is

$$a_j(t) - a_j^i(t) = \int d\rho \sum_{|n_1+n_2|\leq j} \sum_{l_1\geq|n_1|} \sum_{l_2\geq|n_2|} a_{j\,\underset{\sim}{l}\,\underset{\sim}{n}}(t,\underset{\sim}{t}) a^i_{j\,\underset{\sim}{l}\,\underset{\sim}{n}}(t,\underset{\sim}{t}), \quad (2.10)$$

where, if all particles have mass m but are not identical,

$$\int d\rho(t,t_1,t_2) = \frac{i}{(2\pi)^5 2^6}\int dt_1\,dt_2 \times \left[\frac{\lambda^{1/2}(t,t_1,t_2)}{t}\right]\left[\frac{\lambda^{1/2}(t_1,m^2,m^2)}{t_1}\right]\left[\frac{\lambda^{1/2}(t_2,m^2,m^2)}{t_2}\right] \quad (2.11)$$

with the integration region defined by $\lambda \geq 0$, for each of the three λ functions.

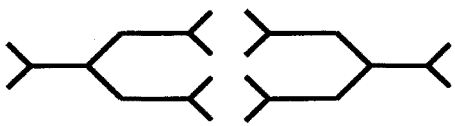

Fig. 2.5. Hexagraph contributions to the unitarity integral.

Temporarily ignoring signature problems, the continuation to complex j for the hexagraph contributions of Fig. 2.5 is given by

$$\sum_{\substack{n_1\geq 0, n_2\geq 0\\ j\geq n_1+n_2}} \to -\frac{\sin\pi j}{2^2}\int_{C_j} \frac{dn_1\,dn_2}{\sin\pi n_1 \sin\pi n_2 \sin\pi(j-n_1-n_2)}, \quad (2.12)$$

where the integration contour is defined so that, for $j \sim -1/2$, $C_j \equiv [n_r = -1/4 + i\nu_r, -\infty < \nu_r < \infty, r = 1,2]$.

We consider the contribution of Regge poles as illustrated in Fig. 2.6.

Fig. 2.6. Regge poles in the production amplitude.

We consider, specifically, $l_1 = n_1$ and $l_2 = n_2$. Writing

$$a_{jn_1n_1n_2n_2}(t,t_1,t_2) = A_{\alpha_1\alpha_2}\frac{1}{[l_1-\alpha_1][l_2-\alpha_2]}\beta_1\beta_2 \quad \alpha_i = \alpha(t_i), \quad (2.13)$$

utilizing two-particle unitarity, and picking out the nonsense pole at $j = n_1 + n_2 - 1$ gives

$$a_j - a_j^i = -\frac{\sin \pi j}{2^2 \pi} \int d\tilde{\rho} \int_{C_j} \frac{dn_1 dn_2}{\sin \pi n_1 \sin \pi n_2 (j - n_1 - n_2 + 1)} \times \frac{\underset{\sim}{A}_\alpha \underset{\sim}{A}^i_\alpha}{(n_1 - \alpha_1)(n_2 - \alpha_2)}, \tag{2.14}$$

where now

$$\int d\tilde{\rho} = \frac{i}{2^5 \pi^3} \int dt_1 dt_2 \left[\frac{\lambda^{1/2}(t, t_1, t_2)}{t} \right]. \tag{2.15}$$

Using the threshold behavior

$$\underset{\sim}{A}_\alpha \underset{\lambda \to 0}{\sim} \left[\frac{\lambda(t, t_1, t_2)}{t} \right]^{(j - \alpha_1 - \alpha_2)}, \tag{2.16}$$

we obtain

$$a_j - a_j^i = -i \frac{\sin \pi j}{2^7 \pi^3} \int \frac{dt_1 dt_2}{\lambda^{1/2}(t, t_1, t_2)} \underset{\sim}{A}_\alpha \underset{\sim}{A}^i_\alpha \times \frac{1}{\sin \pi \alpha_1 \sin \pi \alpha_2 (j - \alpha_1 - \alpha_2 + 1)} + \ldots . \tag{2.17}$$

This leads to the two-reggeon branch-point at $j = 2\alpha(t/4) - 1$ generated by

$$j = \alpha(t_1) + \alpha(t_2) - 1, \qquad \lambda(t, t/4, t/4) = 0. \tag{2.18}$$

Since

$$\int \frac{dt_1 dt_2}{\lambda^{1/2}(t, t_1, t_2)} = 2 \int d^2 k, \tag{2.19}$$

the two-reggeon contribution can naturally be written as a *transverse momentum integral.* The *threshold behavior* (2.16) *at the nonsense point* $j = n_1 + n_2 - 1$ is crucial for this. Specializing to $j \sim 1$, taking $\alpha(t) = 1 + \Delta(t) = 1 + \alpha' t + \ldots$ (and absorbing factors of α' in $\underset{\sim}{A}_\alpha$ and $\underset{\sim}{A}^*_\alpha$), gives for the two-reggeon discontinuity

$$\delta_\omega \left\{ a_\omega \right\} = \frac{1}{2^3 \pi^2} \int \frac{d^2 k}{k^2 (k - q)^2} \underset{\sim}{A}_\alpha \underset{\sim}{A}^*_\alpha \delta(\omega - \Delta_1 - \Delta_2). \tag{2.20}$$

Comparing with (1.1) it is clear that introducing a general 2-2 reggeon interaction will lead to a generalized form of the BFKL equation.

The above analysis of the two-reggeon cut generalizes straightforwardly to the analysis of the N-reggeon cut — which originates from a nonsense state of N-reggeons *i.e.* $j = \sum_{r=1}^{N} \alpha_r - N + 1$. A self-contained set of reggeon unitarity equations can be written [8, 9] for multireggeon scattering amplitudes. All the multireggeon discontinuity formulae can be written in terms of transverse momentum integrals. We emphasize that this is a property of the phase-space generating the branch-point and is not a perturbative result.

Until this point we have effectively ignored signature in our discussion of the two-reggeon cut. However, for the branch-point to actually be generated there must be no "nonsense-zero" of $A_{\underset{\sim}{\alpha}}$ at $j = \alpha_1 + \alpha_2 - 1$. The dispersion integral representation for partial-wave amplitudes implies that *odd-signature amplitudes have such zeros* and so the cut appears only in the even signature amplitude.

2.2. Reggeization

Before specializing to a gauge theory we consider, in general, the "two-reggeon contribution" in the odd-signature channel that (in the gauge theory case) will contain the reggeized gluon. We again consider Regge poles in the four-particle unitarity integral as illustrated in Fig. 2.6. Before allowing for (square-root) nonsense zeros the j-plane contribution is (with signature effects now included)

$$\frac{\pi}{2}\sin\frac{\pi}{2}(j-1)\int d\tilde{\rho}\frac{A_{\underset{\sim}{\alpha}}A^{*}_{\underset{\sim}{\alpha}}}{[j-\alpha_1-\alpha_2+1][\sin\frac{\pi}{2}(\alpha_1-1)][\sin\frac{\pi}{2}(\alpha_2-1)]}. \quad (2.21)$$

We focus on the threshold singularity in t, which is generated when

$$\alpha_1 \equiv \alpha(t_1) = 1\,, \qquad \alpha_2 \equiv \alpha(t_2) = 1\,,$$
$$\lambda(t, t_1, t_2) = 0\,. \quad (2.22)$$

We take $\alpha_1 \sim \alpha_2 \sim 1$ and consider the leading t-dependence for $j \sim 1$. Since $j = 1$ is the nonsense point relevant for the phase-space integration, *we obtain a transverse momentum integral — for the leading threshold behavior.* The two-reggeon phase-space gives (for $\omega = j - 1 \sim 0$)

$$\delta_t\{a_\omega(t)\} = \frac{1}{\omega}\delta_{q^2}\left\{J_1(q^2)A_{\underset{\sim}{\alpha}}A^{*}_{\underset{\sim}{\alpha}}\right\}, \quad (2.23)$$

where $J_1(q^2)$ is defined by (1.2). As illustrated in Fig. 2.7,

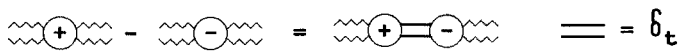

Fig. 2.7. Discontinuity of the 2-2 reggeon amplitude.

the discontinuity formula obtained holds also for the 2-2 reggeon amplitude $A_{\underset{\sim}{\alpha}} \equiv A_{\alpha_1\alpha_2\alpha_3\alpha_4}$ defined at the nonsense point $j = \alpha_1+\alpha_2-1 = \alpha_3+\alpha_4-1$.

We now consider a gauge theory specifically. We input gauge invariance and the color structure of the theory, as we have discussed, by requiring

- Regge pole behavior
- the color structure of the triple Regge vertex
- a nonsense zero
- the Ward identity constraint.

The lowest-order form of $A_{\underset{\sim}{\alpha}}$ is then determined to be

$$A_{\underset{\sim}{\alpha}} = \frac{g^2 \sum_{n=1}^{N} c_{ni_1i_2} c_{ni_3i_4} \omega q^2}{(\omega - \Delta(q^2))} . \tag{2.24}$$

The discontinuity formula of Fig. 2.7 gives directly

$$\Delta(q^2) = g^2 \sum_{j,k} c_{i,j,k}^2 q^2 J_1(q^2) = g^2 N q^2 J_1(q^2) \tag{2.25}$$

which is the familiar leading log form of the gluon trajectory function.

2.3 The BFKL kernel

We consider the six-particle unitarity integral and analyse it with partial-wave amplitudes corresponding to the coupling scheme shown in Fig. 2.8.

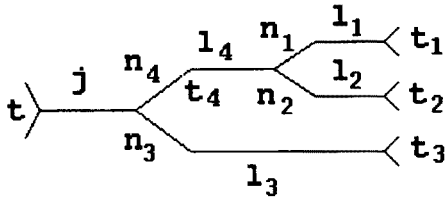

Fig. 2.8. Coupling scheme for the 2-6 production amplitude.

The partial-wave projection of the unitarity integral is

$$a_j(t) - a_j^i(t) = \int d\rho \sum_{|n_3+n_4|\leq j} \sum_{|n_1+n_2|\leq l_4} \sum_{l_1\geq|n_1|} \sum_{l_2\geq|n_2|} \sum_{l_3\geq|n_3|} \sum_{l_4\geq|n_4|} \times a_{j\, \underset{\sim}{l}\, \underset{\sim}{n}}(t, \underset{\sim}{t}) a^i_{j\, \underset{\sim}{l}\, \underset{\sim}{n}}(t, \underset{\sim}{t}) . \tag{2.26}$$

The helicity integrals arising from the continuation to complex j of the helicity sums in (2.26) are (from even signature in j and odd signature in the n_r)

$$\frac{1}{2^8} \sin\frac{\pi}{2} j \int \frac{dn_3 dn_4}{\sin\frac{\pi}{2}(j-n_3-n_4)\sin\frac{\pi}{2}(n_3-1)} \int \frac{dn_1 dn_2}{\sin\frac{\pi}{2}(n_4-n_1-n_2+1)\sin\frac{\pi}{2}(n_1-1)\sin\frac{\pi}{2}(n_2-1)} \tag{2.27}$$

and

$$\int d\tilde{\rho}(t,t_1,t_2,t_3,t_4) = \int_{\lambda(t,t_3,t_4)>0} d\tilde{\rho}(t,t_3,t_4) \int_{\lambda(t_4,t_1,t_2)>0} d\tilde{\rho}(t_4,t_1,t_2) . \tag{2.28}$$

We are interested in the three-particle threshold generated by Regge poles at $n_i = \alpha_i, i = 1,2,3$ when

$$\alpha_1 = \alpha_2 = \alpha_3 = 1 , \qquad \lambda(t_4,t_1,t_2) = \lambda(t,t_3,t_4) = 0 . \tag{2.29}$$

and in the two reggeon cut generated by Regge poles at $n_3 = \alpha_3$ and $n_4 = \alpha_4$ combining with the nonsense pole at $j = n_3 + n_4 - 1$. A nonsense zero prevents a two reggeon cut involving α_1 and α_2 from occurring in the l_4 channel and so no three reggeon cut is generated in the overall j-plane. Nevertheless, for $j \sim 1$ we have

$$\alpha_4 \sim j - \alpha_3 + 1 \sim 2 - \alpha_3 \sim 1 \sim \alpha_1 + \alpha_2 - 1 \tag{2.30}$$

and so the nonsense condition $l_4 = n_4 = n_1 + n_2 - 1$ is satisfied (even though no two reggeon cut is generated). This second condition holds in addition to the $j = n_3 + n_4 - 1$ nonsense condition required for the Regge cut. Since both conditions hold, threshold factors combine to give the right Jacobian factors to change to transverse momentum variables. (This implies that in the following derivation, *the BFKL kernel arises entirely from nonsense states.*) The three-particle discontinuity is then

$$\delta_t \{a_\omega(t)\} = \delta_{q^2} \left\{ J_2(q^2) A_{\underset{\sim}{\alpha}} A^*_{\underset{\sim}{\alpha}} \right\} , \tag{2.31}$$

where

$$J_2(q^2) = \frac{1}{(16\pi^3)^2} \int \frac{d^2k_1 d^2k_3}{k_1^2 k_3^2 (q-k_1-k_3)^2} \,. \tag{2.32}$$

There is a factor of ω^{-1} missing compared to (2.23) because we have extracted nonsense zeroes from the amplitudes.

The lowest-order two-particle/three-reggeon amplitude is determined by factorization. Since $n_4 = (j - \alpha_3 + 1)$ and $(n_4 - \alpha_4) = (\omega - \Delta_3 - \Delta_4)$ we have

$$A_{\underset{\sim}{\alpha}} = \quad \sim \frac{R_L g c_{ijk}}{\omega - \Delta_3 - \Delta_4} \,, \tag{2.33}$$

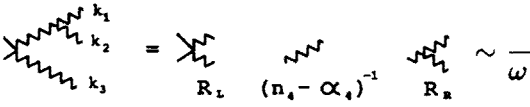

where R_R is the triple reggeon vertex (except that since we have extracted a nonsense zero there is no momentum factor) and R_L is an external vertex which we can take to be a constant carrying zero color *i.e.* we write $R_L = \delta_{ij}$.

Working to $O(g^2)$ in the overall discontinuity and summing over colors we obtain

$$\begin{aligned} \delta_{q^2}\Big\{a_j(q^2)\Big\} = & \\ & \frac{g^2 N}{(16\pi^3)^2} \delta_{q^2} \left\{ \int \frac{d^2k_1 d^2k_3}{k_1^2 k_3^2 (q-k_1-k_3)^2} \frac{1}{(\omega - \alpha' k_3^2 - \alpha'(q-k_3)^2)^2} \right\} \\ & = \frac{g^2 N}{(16\pi^3)} \delta_{q^2} \left\{ \int \frac{d^2k_3}{k_3^2} \frac{J_1((q-k_3)^2)}{(\omega - \alpha' k_3^2 - \alpha'(q-k_3)^2)^2} \right\} . \end{aligned} \tag{2.34}$$

This is the discontinuity of the reggeon diagram shown in Fig. 2.10

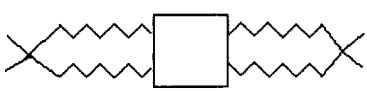

Fig. 2.10. A reggeon diagram.

if the reggeon interaction is the disconnected part of the BFKL kernel.

We must also consider the off-diagonal product of reggeon diagrams shown in Fig. 2.11.

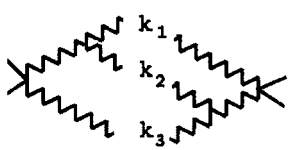

Fig. 2.11. An off-diagonal product of reggeon diagrams.

The right-hand amplitude has a simple form in the partial-wave coupling scheme illustrated in Fig. 2.12. Unfortunately, this partial-wave projection is quite distinct and it is non-trivial to express the new amplitude in the coupling scheme of Fig. 2.8.

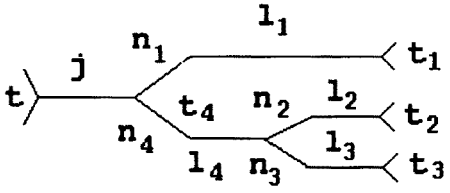

Fig. 2.12. Alternative coupling scheme.

However, if we consider the leading threshold behavior at $t = q^2 = 0$, there is a simplification. To obtain $q^2 = 0$ from three "massless" particles, *i.e.* with $k_i^2 = 0$, $i = 1, 2, 3$, *all three momenta must be parallel.* This implies that *in this special case* the relevant variables of Figs 2.8 and 2.12 degenerate. The helicities of the three particles can be identified, the angles conjugate to j and n_4 can essentially be identified within each scheme and also in the two schemes. In this special kinematic configuration we can write

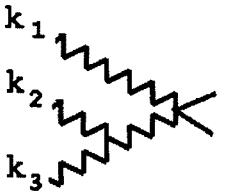

$$\sim \frac{R_L R_R}{\omega - \Delta_1^* - \Delta_{23}^*}, \tag{2.35}$$

where $\Delta_{23} = \alpha'(k_2 + k_3)^2$, $R_R = \delta_{ij}$ and R_L is the triple reggeon vertex.

Combining (2.35) and (2.33) and inserting in (2.31) we again obtain a reggeon diagram of the form of Fig. 2.10. Adding the two possible off-diagonal products we obtain the forward connected BFKL kernel (1.3). The sign is determined by a detailed discussion of the helicities of the reggeons involved [6]. The remaining $(k_1 + k_2)^2$ component has no discontinuity in q^2 and can not be determined by unitarity. It is immediately determined as the first correction away from $q^2 = 0$ once we impose the Ward identity constraint that is our input of gauge invariance. Therefore the full, conformally invariant, BFKL kernel is determined by the combination of t-channel unitarity and Ward identity constraints.

2.4. $O(g^4)$ 2-2 reggeon interactions

We study the eight-particle intermediate state and consider the reggeon contributions shown in Fig. 2.13.

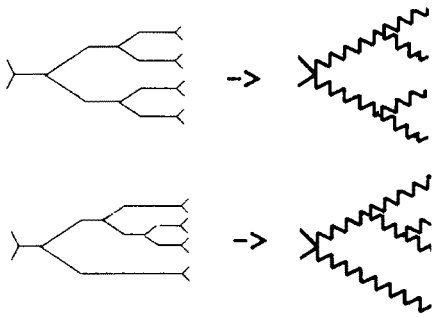

Fig. 2.13. Reggeon contributions to eight-particle unitarity.

Naively we might expect the previous analysis to generalize straightforwardly as illustrated in Fig.2.14.

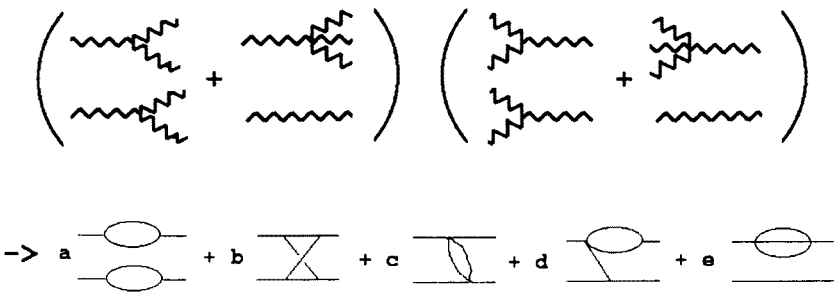

Fig. 2.14. Reggeon interactions.

This would be the kernel given by the reggeon diagram analysis. The coefficients a, b, c, d, e are determined by the Ward identity and infra-red finiteness constraints and might be expected to emerge simply from the unitarity analysis. It is not so simple. We can summarize the subtleties as follows.

(i) The diagram (with coefficient) a is not present, it can be reduced to a sum of reggeization contributions. In fact this diagram requires a minimum rapidity cut-off for it is definition.

(ii) c, d and e all involve the 1-3 reggeon coupling (which in principle) could be zero. As a result nonsense conditions do not follow and only the

combination of infra-red finiteness and Ward identity constraints implies that all the diagrams are present as transverse momentum integrals in the infra-red region.

(iii) In the infra-red region, diagram *b directly generates a transverse momentum integral* but only *for the leading threshold behavior in the reggeon mass variables.* Also, the product of distinct partial-wave amplitudes involved generates an *overall normalization ambiguity in transforming from one partial-wave to the other.*

We shall see in the next Section that the component of diagram *b* that emerges as most unambiguously defined indeed has special importance.

3. Properties of the $O(g^4)$ kernels

We now return from the unitarity analysis to the kernels that we initially constructed using reggeon diagrams [12]. We first discuss the properties of these kernels and then return to the issue of how they contribute as higher-order corrections to the BFKL kernel. As we outlined above, and is described in more detail in [12], the *construction procedure* is to use reggeon diagrams to generate all possible transverse momentum diagrams and then use Ward identity and infra-red finiteness constraints to determine the relative coefficients.

3.1. The $O(g^4)$ 2-4 kernel

We discuss this only briefly. The complete 2-4 kernel is given by

$$K^{(4)}_{2,4}(k_1,k_2,k_3,k_4,k_5,k_6) = \sum_{1<->2} 2\pi^3 k_2^2 \Big(\delta^2(k_2-k_6)K^{(4)}_{1,3}(k_1,k_3,k_4,k_5)$$
$$+\delta^2(k_2-k_5)K^{(4)}_{1,3}(k_1,k_3,k_4,k_6)+\delta^2(k_2-k_4)K^{(4)}_{1,3}(k_1,k_3,k_5,k_6)$$
$$+\delta^2(k_2-k_3)K^{(4)}_{1,3}(k_1,k_4,k_5,k_6)\Big) - K^{(4)}_{2,4}(k_1,k_2,k_3,k_4,k_5,k_6)_c\,, \qquad (3.1)$$

where the first four terms are disconnected components and involve $K^{(4)}_{1,3}(k,k_1,k_2,k_3)$, which is given by the reggeon diagrams of Fig. 3.1

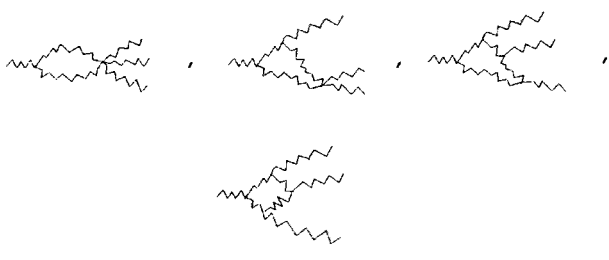

Fig. 3.1. Reggeon diagrams giving $K^{(4)}_{1,3}$.

and can be written as

$$K^{(4)}_{1,3}(k,k_1,k_2,k_3) = \frac{1}{(2\pi)^3}\int \frac{d^2k_1}{k_1^2}\frac{d^2k_2}{k_2^2}k^2\delta^2(k-k_1-k_2) \times K^{(4)}_{2,3}(k_1,k_2,k_3,k_4,k_5)\,, \tag{3.2}$$

where

$$g^{-4}K^{(4)}_{2,3}(k_1,k_2,k_3,k_4,k_5) = \sum_{1<->2}\left((k_1+k_2)^2 - \left(\frac{k_1^2(k_4+k_5)^2}{(k_1-k_3)^2} + \frac{k_1^2(k_3+k_5)^2}{(k_1-k_4)^2} + \frac{k_1^2(k_3+k_4)^2}{(k_1-k_5)^2}\right) + \frac{1}{3}\left(\frac{k_1^2k_5^2}{(k_2-k_5)^2} + \frac{k_1^2k_4^2}{(k_2-k_4)^2} + \frac{k_1^2k_3^2}{(k_2-k_3)^2}\right) + \frac{2}{3}\left(\frac{k_1^2k_2^2k_4^2}{(k_1-k_3)^2(k_2-k_5)^2} + \frac{k_1^2k_2^2k_5^2}{(k_1-k_4)^2(k_2-k_3)^2} + \frac{k_1^2k_2^2k_3^2}{(k_1-k_5)^2(k_2-k_4)^2}\right)\right). \tag{3.3}$$

$K^{(4)}_{2,4}(k_1,..,k_6)_c$ is the connected part of the kernel and is generated by the reggeon diagrams shown in Fig. 3.2

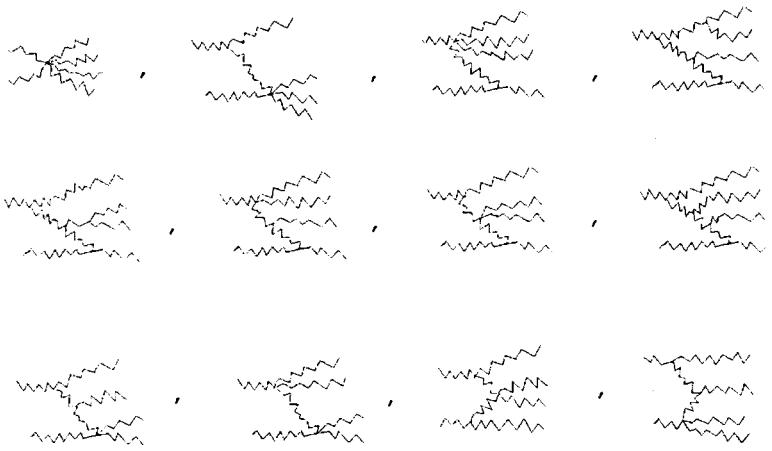

Fig. 3.2. Reggeon diagrams for the connected 2-4 reggeon kernel.

The resulting transverse momentum diagrams have already appeared in Fig. 1.7. In detail we have

$$
\begin{aligned}
g^{-4}K^{(4)}_{2,4}(k_1,k_2,k_3,k_4,k_5,k_6)_c = \sum_{1<->2}\Bigg(& (k_1+k_2)^2 - \Bigg(\frac{k_1^2(k_4+k_5+k_6)^2}{(k_1-k_3)^2} \\
& + \frac{k_1^2(k_3+k_5+k_6)^2}{(k_1-k_4)^2} + \frac{k_1^2(k_3+k_4+k_6)^2}{(k_1-k_5)^2} + \frac{k_1^2(k_3+k_4+k_5)^2}{(k_1-k_6)^2} \Bigg) \\
& - \frac{1}{4}\left(\frac{k_1^2k_3^2}{(k_2-k_3)^2} + \frac{k_1^2k_4^2}{(k_2-k_4)^2} + \frac{k_1^2k_5^2}{(k_2-k_5)^2} + \frac{k_1^2k_6^2}{(k_2-k_6)^2} \right) \\
& + \frac{1}{2}\Bigg(\frac{k_1^2(k_5+k_6)^2}{(k_2-k_5-k_6)^2} + \frac{k_1^2(k_5+k_4)^2}{(k_2-k_5-k_4)^2} + \frac{k_1^2(k_4+k_6)^2}{(k_2-k_4-k_6)^2} \\
& + \frac{k_1^2(k_3+k_6)^2}{(k_2-k_3-k_6)^2} + \frac{k_1^2(k_5+k_3)^2}{(k_2-k_5-k_3)^2} + \frac{k_1^2(k_3+k_4)^2}{(k_2-k_3-k_4)^2} \Bigg) \\
& + \frac{1}{2}\Bigg(\frac{k_1^2k_2^2(k_4+k_5)^2}{(k_1-k_3)^2(k_2-k_6)^2} + \frac{k_1^2k_2^2(k_3+k_5)^2}{(k_1-k_4)^2(k_2-k_6)^2} + \frac{k_1^2k_2^2(k_3+k_4)^2}{(k_1-k_5)^2(k_2-k_6)^2} \\
& + \frac{k_1^2k_2^2(k_3+k_6)^2}{(k_1-k_4)^2(k_2-k_5)^2} + \frac{k_1^2k_2^2(k_4+k_6)^2}{(k_1-k_3)^2(k_2-k_5)^2} + \frac{k_1^2k_2^2(k_5+k_6)^2}{(k_1-k_3)^2(k_2-k_4)^2} \Bigg) \\
& - \frac{1}{4}\Bigg(\frac{k_1^2k_2^2k_4^2}{(k_1-k_3)^2(k_2-k_5-k_6)^2} + \frac{k_1^2k_2^2k_5^2}{(k_1-k_3)^2(k_2-k_4-k_6)^2} \\
& + \frac{k_1^2k_2^2k_6^2}{(k_1-k_3)^2(k_2-k_4-k_5)^2} + \frac{k_1^2k_2^2k_3^2}{(k_1-k_4)^2(k_2-k_5-k_6)^2} \\
& + \frac{k_1^2k_2^2k_5^2}{(k_1-k_4)^2(k_2-k_3-k_6)^2} + \frac{k_1^2k_2^2k_6^2}{(k_1-k_4)^2(k_2-k_3-k_5)^2} \\
& + \frac{k_1^2k_2^2k_4^2}{(k_1-k_5)^2(k_2-k_3-k_6)^2} + \frac{k_1^2k_2^2k_3^2}{(k_1-k_5)^2(k_2-k_4-k_6)^2} \\
& + \frac{k_1^2k_2^2k_6^2}{(k_1-k_5)^2(k_2-k_4-k_3)^2} + \frac{k_1^2k_2^2k_4^2}{(k_1-k_6)^2(k_2-k_5-k_3)^2} \\
& + \frac{k_1^2k_2^2k_5^2}{(k_1-k_6)^2(k_2-k_4-k_3)^2} + \frac{k_1^2k_2^2k_3^2}{(k_1-k_6)^2(k_2-k_4-k_5)^2} \Bigg)\Bigg). \qquad (3.4)
\end{aligned}
$$

It is straightforward to check [12] that all the Ward identity constraints are satisfied by $K^{(4)}_{2,4}$. This vertex is essentially that calculated directly by Bartels and Wüsthoff [17], although to obtain precisely the same result it

is necessary to include the relevant color factors correctly. Note that the existence of $K_{2,4}^{(4)}$ immediately implies that there is no closed BFKL equation at $O(\alpha_s^2)$. To obtain such an equation we have to artificially restrict the discussion to 2-2 reggeon interactions.

3.2. The $O(g^4)$ 2-2 kernel

As we discussed earlier, reggeon diagrams containing four-reggeon intermediate states generate the sum of transverse momentum diagrams for the 2-2 kernel shown in Fig. 1.7 and give five kinematically distinct terms.

$$\frac{1}{(g^2N)^2}K_{2,2}^{(4n)}(k_1,k_2,k_3,k_4) = K_0^{(4)} + K_1^{(4)} + K_2^{(4)} + K_3^{(4)} + K_4^{(4)} \quad (3.5)$$

with

$$K_0^{(4)} = \sum k_1^4 k_2^4 J_1(k_1^2) J_1(k_2^2)(16\pi^3)\delta^2(k_2 - k_3)\,, \quad (3.6)$$

$$K_1^{(4)} = -\frac{2}{3}\sum k_1^4 J_2(k_1^2) k_2^2 (16\pi^3)\delta^2(k_2 - k_3)\,, \quad (3.7)$$

$$K_2^{(4)} = -\sum\left(\frac{k_1^2 J_1(k_1^2) k_2^2 k_3^2 + k_1^2 k_3^2 J_1(k_4^2) k_4^2}{(k_1 - k_4)^2}\right), \quad (3.8)$$

$$K_3^{(4)} = \sum k_2^2 k_4^2 J_1((k_1 - k_4)^2)\,, \quad (3.9)$$

and

$$K_4^{(4)} = \frac{1}{2}\sum k_1^2 k_2^2 k_3^2 k_4^2 I(k_1,k_2,k_3,k_4)\,, \quad (3.10)$$

where $J_1(k^2)$ is defined by (1.2) and

$$J_2(k^2) = \frac{1}{16\pi^3}\int d^2q \frac{1}{(k-q)^2} J_1(q^2)\,, \quad (3.11)$$

and

$$I(k_1,k_2,k_3,k_4) = \frac{1}{16\pi^3}\int d^2p \frac{1}{p^2(p+k_1)^2(p+k_1-k_4)^2(p+k_3)^2}\,. \quad (3.12)$$

We can demonstrate, diagrammatically, that the Ward identity infrared finiteness constraints are satisfied as follows. For an external k_i-line

- $k_i \to 0$ gives zero if the line carrying k_i is the single line of a 1-2, 2-1, or 1-1 vertex,
- in general, $k_i \to 0$ gives the subdiagram obtained by removing the line carrying k_i.

Infra-red divergences occur when the momentum k_i of an internal line vanishes. If we use a mass regulation, then, as $m^2 \to 0$, this gives

$$\int d^2k_i \frac{f(k_i)}{(k_i^2+m^2)} \to \frac{1}{2}\int \frac{dk_i^2}{(k_i^2+m^2)} \int_0^{2\pi} d\theta f(0) \to \pi \log m^2 f(0), \quad (3.13)$$

where (apart from a factor of $(16\pi^3)^{-1}$) $f(0)$ is obtained from the original diagram by removing the line carrying k_i.

The Ward identity constraint is satisfied by the relation

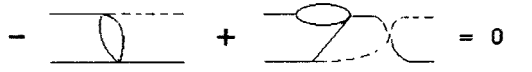

(3.14)

(with the notation $- - - \equiv k_i \to 0$) and so determines the relative weight of K_2 and K_3. There are two infra-red finiteness requirements, leading to three constraints that determine the relative weights of the remaining components. First we require that the connected part of the kernel is infra-red finite before integration. This gives

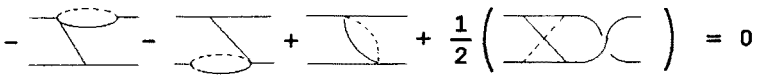

(3.15)

and determines K_4 relative to K_2 and K_3. Taking the Ward identity zeroes into account, infra-red finiteness after integration requires cancellation, by the disconnected parts, of two divergences due to the connected part. First the poles of K_2 require the cancellation

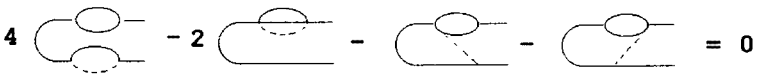

(3.16)

Secondly K_3 generates a divergence, when both exchanged lines carry zero transverse momentum, which requires the cancellation

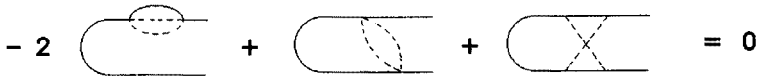

(3.17)

This last constraint determines $K_1^{(4)}$ relative to $K_2^{(4)} + K_3^{(4)} + K_4^{(4)}$ and the previous constraint then determines the relative weight of $K_0^{(4)}$.

The most complicated part of $K^{(4n)}$ is clearly $K_4^{(4)}$ since it contains the box diagram I_4. Using the notation illustrated in Fig. 3.3

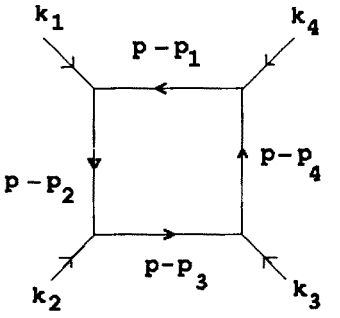

Fig. 3.3. Notation for the box diagram

we write

$$I_4(p_1, p_2, p_3, p_4, m^2) = \int d^2p \Pi_{i=1}^4 \frac{1}{[(p - p_i)^2 - m^2]},$$

I_4 can be evaluated [16] as a sum of logarithms, *i.e.*

$$I_4 = \sum_{j<k} A_{jk} F_{jk}, \tag{3.18}$$

where the A_{jk} are "tree-diagrams" obtained by putting internal lines j and k on-shell and

$$F_{jk} = \frac{i\pi}{\lambda^{1/2}(p_{jk}^2, m^2, m^2)} \mathrm{Log}\left[\frac{p_{jk}^2 - 2m^2 - \lambda^{1/2}(p_{jk}^2, m^2, m^2)}{p_{jk}^2 - 2m^2 + \lambda^{1/2}(p_{jk}^2, m^2, m^2)}\right] \tag{3.19}$$

with

$$p_{jk} = (p_j - p_k)^2. \tag{3.20}$$

To obtain explicit expressions for the A_{jk} requires introducing dual vectors to the p_{jk} and leads to

$$A_{jk} = \frac{a_{jk}}{b_{jk}}, \tag{3.21}$$

where, *e.g.*

$$a_{12} = \left[k_1 \cdot k_2{}^2 - k_1{}^2 k_2{}^2\right] \times \Big[k_1 \cdot k_2{}^2 - k_1 \cdot k_2\, k_1 \cdot k_3 - k_1{}^2 k_2{}^2 + k_1{}^2\, k_2 \cdot k_3 + (k_1 \cdot k_2 + k_2{}^2)(k_1 \cdot k_2 - k_1 \cdot k_3 + k_2{}^2 - 2\, k_2 \cdot k_3 + k_3{}^2)\Big], \tag{3.22}$$

$$b_{12} = \left[-k_1 \cdot k_2{}^2 + k_1{}^2 k_2{}^2 + (k_1 \cdot k_2 + k_2{}^2)^2\right] \times \Big[-(k_1 \cdot k_2{}^2 - k_1 \cdot k_2 k_1 \cdot k_3 - k_1{}^2 k_2{}^2 + k_1{}^2 k_2 \cdot k_3)^2 + (k_1 \cdot k_2{}^2 - k_1{}^2 k_2{}^2))(k_1 \cdot k_2 - k_1 \cdot k_3 + k_2{}^2 - 2k_2 \cdot k_3 + k_3{}^2)^2\Big]. \tag{3.23}$$

In this way we obtain the box diagram as a sum of six logarithms of two types:

(1) external line "reggeon mass" thresholds, → four logarithms.
(2) "s" and "t" thresholds, → two logarithms.

The complete kernel can then be written in terms of logarithms with rational polynomial factors. (In fact a greatly simplified expression can be found in [18]).

3.3. The $O(g^4)$ parton kernel

For parton evolution, we require only the much simpler "forward" kernel

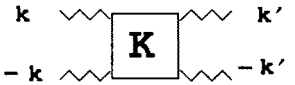

$$= K_{2,2}^{(4n)}(k, -k, k', -k') \equiv K^{(4)}(k, k'). \tag{3.24}$$

In the forward direction it is straightforward to combine the type (2) logarithms from the box with the logarithms of the connected components $K_2^{(4)}$ and $K_3^{(4)}$, giving

$$K^{(4)}(k,k')_c \underset{m^2 \to 0}{\longrightarrow} \frac{1}{8\pi^2}\left(\frac{k^2 k'^2}{(k-k')^2}\mathrm{Log}\left[\frac{(k-k')^4}{k^2 k'^2}\right] + \frac{k^2 k'^2}{(k+k')^2}\mathrm{Log}\left[\frac{(k+k')^4}{k^2 k'^2}\right]\right) - \left(\mathcal{K}_2\right), \tag{3.25}$$

where

$$\mathcal{K}_2 = \frac{1}{4\pi^2}\frac{k^2 k'^2 (k^2 - k'^2)}{(k+k')^2 (k-k')^2} \mathrm{Log}\left[\frac{k^2}{k'^2}\right]$$

is *separately infra-red finite* as $m^2 \to 0$ and contains only the type (1) logarithms, *i.e.* the external reggeon mass thresholds. $\mathcal{K}_2$ will be very important in the following. *It is the part of the box-diagram that emerged as a well-defined transverse momentum integral contribution via the unitarity analysis.*

To obtain the full set of eigenvalues of $K^{(4)}$ we first show diagrammatically that

$$K^{(4)} = \frac{1}{4}(K_{\mathrm{BFKL}})^2 - \mathcal{K}_2\,, \tag{3.27}$$

where $K_{\mathrm{BFKL}} = K_{\mathrm{BFKL}}(k, -k, k', -k')$ is given by (1.4). We have

$(K_{\mathrm{BFKL}})^2 =$ 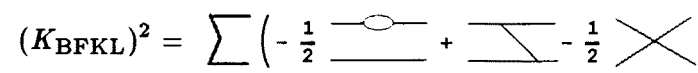 (3.28)

$=$ 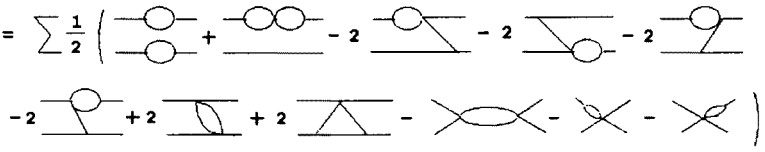 (3.29)

Using the forward identities

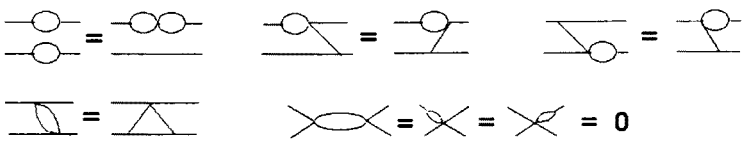 (3.30)

then gives

$(K_{\mathrm{BFKL}})^2 =$ 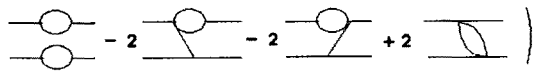 (3.31)

and (3.27) follows.

3.4. Eigenvalues and holomorphic factorization

We use the complete set of orthogonal eigenfunctions

$$\phi_{\nu,n}(k) = (k^2)^{1/2+i\nu} \mathrm{e}^{in\theta} \qquad \nu \in (-\infty, \infty)\,, \quad n = 0, \pm 1, \pm 2, \ldots\,, \tag{3.32}$$

$k = (|k|\cos\theta, |k|\sin\theta)$. The eigenvalues of K_{BFKL} are $(Ng^2/2\pi^2)\chi(\nu,n)$, where

$$\chi(\nu,n) = \psi(1) - \mathrm{Re}\,\psi\left(\frac{|n|+1}{2} + i\nu\right) \tag{3.33}$$

with $\psi(x) = \frac{d}{dx}\ln\Gamma(x)$. From (3.27) the eigenvalue spectrum of $K^{(4)}$ is given by $N^2g^4\mathcal{E}(\nu,n)$ where

$$\mathcal{E}(\nu,n) = \frac{1}{\pi}[\chi(\nu,n)]^2 - \Lambda(\nu,n)\,. \tag{3.34}$$

and $\Lambda(\nu,n)$ are the eigenvalues of $\mathcal{K}_2$.

To find the $\Lambda(\nu,n)$ we use the dimensionally regularized form of $\mathcal{K}_2$, *i.e.*

$$\mathcal{K}_2^D(k,k') = \frac{1}{2\pi^2(D-2)}\frac{k^2k'^2(k^2-k'^2)}{(k+k')^2(k-k')^2}\left((k^2)^{D/2-1} - (k'^2)^{D/2-1}\right). \tag{3.35}$$

We first evaluate

$$I_\theta[n] \equiv \int_0^{2\pi} d\theta' \frac{\mathrm{e}^{in\theta'}}{1 - z(k,k')sin^2\,(\theta-\theta')}\,,$$

$$z[k,k'] = -\frac{4k^2k'^2}{(k^2-k'^2)^2}\,, \tag{3.36}$$

where $\cos\theta = k\cdot\hat{x}$ and $\cos\theta' = k'\cdot\hat{x}$. We get by residue (for $n > -1$)

$$\begin{aligned} I_\theta[n] &= -4i\mathrm{e}^{in\theta}\oint dw \frac{w^{n+1}}{zw^4 + 2(2-z)w^2 + z} \\ &= 2\pi\delta_{n,2M}\mathrm{e}^{in\theta}\left(\frac{k^2-k'^2}{k^2+k'^2}\right)\left[\left(\frac{k}{k'}\right)^n\Theta[k'-k] - \left(\frac{k'}{k}\right)^n\Theta[k-k']\right]. \end{aligned} \tag{3.37}$$

$2M$ is an even integer — this will be important in the following.

It is then straightforward to show that

$$\int \frac{d^Dk'}{(k')^2}\mathcal{K}_2^D(k,k')\phi_{\nu,n}(k') = \Lambda(\nu,n)\phi_{\nu,n}(k)\,, \tag{3.38}$$

where, as $D \to 2$,

$$\begin{aligned} \Lambda(\nu,n) \to \frac{1}{2\pi^2(D-2)}\Big(&\beta\big(\tfrac{|n|}{2} + \tfrac{D}{2} + \nu - \tfrac{1}{2}\big) \\ &- \beta\big(\tfrac{|n|}{2} - \tfrac{D}{2} - \nu + \tfrac{3}{2}\big) - \big(\beta\big(\tfrac{|n|}{2} + D + \nu - \tfrac{3}{2}\big) \\ &+ \beta\big(\tfrac{|n|}{2} - D - \nu + \tfrac{5}{2}\big)\big)\Big)\,, \end{aligned} \tag{3.39}$$

$\beta(x)$ is the incomplete beta function, *i.e.*

$$\begin{aligned}\beta(x) &= \int_0^1 dy y^{x-1}[1+y]^{-1} \\ &= \frac{1}{2}\left(\psi(\frac{x+1}{2}) - \psi(\frac{x}{2})\right),\end{aligned} \tag{3.40}$$

and so, at $D = 2$,

$$\Lambda(\nu, n) = -\frac{1}{4\pi}\left(\beta'\left(\frac{|n|+1}{2} + i\nu\right) + \beta'\left(\frac{|n|+1}{2} - i\nu\right)\right), \tag{3.41}$$

where we can write

$$\beta'(x) = \frac{1}{4}\left(\psi'\left(\frac{x+1}{2}\right) - \psi'\left(\frac{x}{2}\right)\right) \tag{3.42}$$

with

$$\psi'(z) = \sum_{r=0}^{\infty} \frac{1}{(r+z)^2}\,. \tag{3.43}$$

Using (3.42) we can show that the $\Lambda(\nu, n)$ have the important property of *holomorphic factorization* that is very closely related to conformal symmetry [19]. That is we can write

$$\Lambda(\nu, n) = \mathcal{G}\left[m(1-m)\right] + \mathcal{G}\left[\tilde{m}(1-\tilde{m})\right], \tag{3.44}$$

where $m = 1/2 + i\nu + n/2$ and $\tilde{m} = 1/2 + i\nu - n/2$ are conformal weights. We use

$$\begin{aligned}16\pi\Lambda(\nu, n) &= -4\left(\beta'(m) + \beta'(1-\tilde{m})\right) \\ &= \psi'\left(\frac{m+1}{2}\right) - \psi'\left(\frac{m}{2}\right) + \psi'\left(\frac{2-\tilde{m}}{2}\right) - \psi'\left(\frac{1-\tilde{m}}{2}\right) \\ &= \sum_{r=0}^{\infty} \frac{1}{(r+\frac{3}{4}+\frac{n}{4}+\frac{i\nu}{2})^2} - \sum_{r=0}^{\infty} \frac{1}{(r+\frac{1}{4}+\frac{n}{4}+\frac{i\nu}{2})^2} \\ &+ \sum_{r=0}^{\infty} \frac{1}{(r+\frac{3}{4}+\frac{n}{4}-\frac{i\nu}{2})^2} - \sum_{r=0}^{\infty} \frac{1}{(r+\frac{1}{4}+\frac{n}{4}-\frac{i\nu}{2})^2}\,.\end{aligned} \tag{3.45}$$

We next show that this expression is unchanged if we simultaneously send $m \to 1-m$ and $\tilde{m} \to 1-\tilde{m}$, *i.e.* $n \to -n, \nu \to -\nu$. At this point *it is crucial that* n *is an even integer.* Writing $n = 2M$, we obtain

$$16\pi\Lambda(-\nu,-n) = \sum_{r=0}^{\infty} \frac{1}{(r+\frac{1}{4}+\frac{-M+1}{2}-\frac{i\nu}{2})^2} - \sum_{r=0}^{\infty} \frac{1}{(r+\frac{1}{4}+\frac{-M}{2}-\frac{i\nu}{2})^2} + \sum_{r=0}^{\infty} \frac{1}{(r+\frac{1}{4}+\frac{-M+1}{2}+\frac{i\nu}{2})^2} - \sum_{r=0}^{\infty} \frac{1}{(r+\frac{1}{4}+\frac{-M}{2}+\frac{i\nu}{2})^2}, \tag{3.46}$$

and so

$$\begin{aligned} &16\pi\big(\Lambda(-\nu,-n)-\Lambda(\nu,n)\big) \\ &= \sum_{s=-M}^{-1} \frac{1}{(s+\frac{1}{4}+\frac{M+1}{2}-\frac{i\nu}{2})^2} - \sum_{s=-M}^{-1} \frac{1}{(s+\frac{1}{4}+\frac{M}{2}-\frac{i\nu}{2})^2} \\ &+ \sum_{s=-M}^{-1} \frac{1}{(s+\frac{1}{4}+\frac{M+1}{2}+\frac{i\nu}{2})^2} - \sum_{s=-M}^{-1} \frac{1}{(s+\frac{1}{4}+\frac{M}{2}+\frac{i\nu}{2})^2} \\ &= \sum_{t=-M/2}^{M/2-1} \frac{1}{(t+\frac{3}{4}-\frac{i\nu}{2})^2} - \sum_{t=-M/2}^{M/2-1} \frac{1}{(-t-\frac{1}{4}-\frac{i\nu}{2})^2} \\ &+ \sum_{t=-M/2}^{M/2-1} \frac{1}{(t+\frac{3}{4}+\frac{i\nu}{2})^2} - \sum_{t=-M/2}^{M/2-1} \frac{1}{(-t-\frac{1}{4}+\frac{i\nu}{2})^2} \\ &= 0\,. \end{aligned} \tag{3.47}$$

From this symmetry, we can write

$$\begin{aligned} 16\pi\Lambda(\nu,n) &= -2\Big(\beta'(m)+\beta'(1-m)+\beta'(1-\tilde{m})\Big)+\beta'(\tilde{m})\Big) \\ &\equiv \mathcal{G}\big[m(1-m)\big]+\mathcal{G}\big[\tilde{m}(1-\tilde{m})\big] \end{aligned} \tag{3.48}$$

as required.

We conclude that $\mathcal{K}_2$ shares many of the nice properties of the leading-order BFKL kernel. It is infra-red finite, scale-invariant and has a *new eigenvalue spectrum* satisfying *holomorphic factorization.* It is very interesting to ask whether there is a new conformally invariant, non-forward, kernel associated with $\mathcal{K}_2$. (In fact it is shown in [6] that $\mathcal{K}_2$ is the forward component of a new partial-wave amplitude that appears for the first time

at $O(g^4)$ and in [18] a candidate for the non-forward conformally invariant kernel is constructed.)

3.5 Numerical evaluation

We consider now the numerical significance of the eigenvalues of $K^{(4)}$. The leading eigenvalue is at $\nu = n = 0$, as it is for the $O(g^2)$ kernel. Using the reggeon diagram normalization, the correction to α_0 is given [16], by

$$9g^4 \frac{\mathcal{E}(0,0)}{16\pi^3}. \tag{3.49}$$

Since

$$\begin{aligned} \Lambda(0,0) &= -\frac{1}{2\pi}\beta'\left(\frac{1}{2}\right) \\ &= -\frac{1}{8\pi}\left(\sum_{r=0}^{\infty}\frac{1}{(r+1/4)^2} - \sum_{r=0}^{\infty}\frac{1}{(r+3/4)^2}\right) \\ &= -\frac{1}{8\pi}\left(16 + \frac{16}{25} + \frac{16}{81} + \ldots - \frac{16}{9} - \frac{16}{49} + \ldots\right) \\ &\sim -\frac{1.81}{\pi}, \end{aligned} \tag{3.50}$$

we obtain from $\mathcal{K}_2$ alone

$$\frac{9g^4}{16\pi^3}\Lambda(0,0) \sim -16.3\frac{{\alpha_s}^2}{\pi^2}. \tag{3.51}$$

The complete $K^{(4n)}$ gives

$$\begin{aligned} &\sim \frac{9g^4}{16\pi^4}\left([2\ln 2]^2 - 1.81\right), \\ &\sim \frac{9g^4}{16\pi^4} \times 0.11 \sim \frac{{\alpha_s}^2}{\pi^2}, \end{aligned} \tag{3.52}$$

giving a very small positive effect.

At this point we note that the disconnected part of $K^{(4)}$ contains diagrams, the first kind appearing in (3.31), which can not be interpreted in terms of reggeization effects. Since reggeization is the only consistent interpretation of disconnected pieces, these diagrams can not be present in the full kernel. Elimination of the unwanted diagrams, while retaining scale-invariance, gives [16] uniquely

$$\tilde{K}^{(4)} = K^{(4n)} - \left(K_{\mathrm{BFKL}}\right)^2, \tag{3.53}$$

This is a consistent scale-invariant $O(g^4)$ kernel which can be added to the $O(g^2)$ kernel. In this case, we replace $\mathcal{E}(\nu, n)$ by $\tilde{\mathcal{E}}(\nu, n)$ where

$$\tilde{\mathcal{E}}(\nu, n) = -\frac{3}{\pi}[\chi(\nu, n)]^2 - \Lambda(\nu, n)\,. \tag{3.54}$$

This gives, as a modification of α_0,

$$\begin{aligned} 9g^4 \frac{\tilde{\mathcal{E}}(0,0)}{16\pi^3} &\sim \frac{9g^4}{16\pi^4} \times (-5.76 - 1.81) \\ &\sim -68\frac{{\alpha_s}^2}{\pi^2} \end{aligned} \tag{3.55}$$

which is a substantial negative correction — of the order of 50%.

Unfortunately as we have discussed in the last Section there is, even in the best determined component $\mathcal{K}_2$, an overall normalization uncertainty which reduces the immediate significance of these numerical estimates.

4. The $O(g^4)$ kernel from the s-channel effective action

Kirschner [15] has discussed the relationship of the "t-channel" reggeon diagram construction of non-leading kernels to the "s-channel" multi-Regge effective action [4] derived from the leading-log approximation. The full effective action is written as a sum of components

$$\mathcal{L} = \mathcal{L}_{\text{kin}} + \mathcal{L}_s + \mathcal{L}_p + \mathcal{L}_t\,. \tag{4.1}$$

$\mathcal{L}_t$ contains the triple-gluon vertex for longitudinal gluon fields A_+, A_-, describing "t-channel" exchanged gluons ("s-channel" produced gluons are described by $A_\perp$ fields), *i.e.*

$$\mathcal{L}_t = \frac{ig}{2}\partial\partial^* A_-^a(\partial_+^{-1}A_+T^aA_+) + \partial\partial^* A_+^a(\partial_-^{-1}A_-T^aA_-)\,. \tag{4.2}$$

In momentum space the triple vertex has the form

$$igc_{abc}\frac{(k_1+k_2)^2}{k_{2+}} + (k_2, b) < - > (k_1, c) \tag{4.3}$$

and is, essentially, the three-reggeon vertex that we use to construct reggeon diagrams.

Kirschner has shown that graphs involving triple-gluon vertices can be regarded as reggeon diagrams, *if contributions with s-channel gluons close*

to mass-shell are added. The $O(g^4)$ kernel we have discussed arises from the product of interactions shown in Fig. 4.1

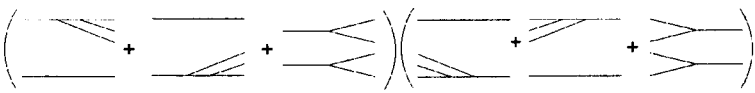

Fig. 4.1. Reggeon interactions from the multi-Regge effective action.

together with additional contributions from s-channel gluons. (This is clearly analogous to the product of reggeon diagrams illustrated in Fig. 2.14.) If the resulting diagrams are written as transverse momentum integrals, the formalism suggests that the original presence of additional rapidity integrations produces both

- an overall normalization uncertainty
- additional (perhaps slowly varying) transverse momentum dependence.

Since these results are completely consistent with our results, the effective lagrangian gives a valuable understanding of the reggeon diagram approximation.

Kirschner also gives an interesting representation for $\mathcal{K}_2$. Introducing complex momenta κ whose real and imaginary parts are the two components of conventional transverse momenta

$$\mathcal{K}_2(\kappa,\kappa') = \frac{2\kappa^2\kappa'^2}{(2\pi)^3}\int d^2\kappa'' \frac{1}{\kappa''(\kappa''-\kappa+\kappa')(\kappa''-\kappa)^*(\kappa''+\kappa')^*} + \text{c.c.}. \tag{4.4}$$

This formalism is used in [18] to construct the non-forward extension of $\mathcal{K}_2$ and is anticipated to be very useful for studying conformal symmetry properties.

5. Conclusions

Used directly, the scale invariant $O(g^4)$ transverse momentum kernel gives a *large reduction of the BFKL small-x behavior of parton distributions.* However, both t-channel unitarity and the multi-Regge effective action imply that the introduction of *scales will modify the normalization* and significantly modify the kernel at large q^2, k^2, k'^2. Indeed the outcome of the non-leading t-channel unitarity that we have outlined in Section 2 can be compactly summarized [6] by writing, for the full kernel $K_{2,2}(q,k,k')$,

$$K_{2,2}(q,k,k') \underset{q^2,k^2,k'^2\to 0}{\longrightarrow} g^2 K_{\text{BFKL}} + O(g^4)(K_{\text{BFKL}})^2 + O(g^4)\mathcal{K}_2\,, \tag{5.1}$$

indicating that both the overall normalization and the relative normalization of the new $\mathcal{K}_2$ kernel to $(K_{\rm BFKL})^2$, are not determined.

A reggeon interaction derived from t-channel unitarity, is necessarily scale-invariant and only an infra-red approximation. Extrapolation away from the infra-red region is controlled by the Ward identity constraints and in [16] we conjecture that these constraints lead to conformal invariance. The BFKL kernel, the triple Regge kernel [17, 12, 20], and the $\mathcal{K}_2$ kernel we have derived, are the only interactions studied so far and existing results are consistent with this conjecture.

In [7] we have outlined a program whereby the scale-dependence of non-leading reggeon amplitudes can be studied via the Ward identity constraints. We hope to study this possibility in the future. Of course, completion of the full $O(\alpha_s^2)$ calculation [3] should greatly clarify the role of scale dependence in the 2-2 kernel. Comparison with the reggeon diagram formalism may then suggest how yet higher-order contributions can be suitably approximated.

We are grateful to J. Bartels, R. Kirschner and L. Lipatov for valuable discussions of this work.

REFERENCES

[1] E.A. Kuraev, L.N. Lipatov, V.S. Fadin, *Sov. Phys. JETP* **45**, 199 (1977); Ya.Ya. Balitsky, L.N. Lipatov, *Sov. J. Nucl. Phys.* **28**, 822 (1978); L.N. Lipatov, in *Perturbative QCD*, ed. A.H. Mueller, World Scientific, Singapore 1989.

[2] J. Bartels, DESY preprint, DESY 91-074 (1991) and *Z. Phys.* **C60**, 471 (1993); *Nucl. Phys.* **B151**, 293 (1979); **B175**, 365 (1980).

[3] V.S. Fadin, L.N. Lipatov, *Nucl. Phys.* **B406**, 259 (1993).

[4] R. Kirschner, L.N. Lipatov, L. Szymanowski, *Nucl. Phys.* **B425**, 579 (1994); *Phys. Rev.* **D51**, 838 (1995); L.N. Lipatov, DESY 95-029, hep-ph/9502308.

[5] L.N. Lipatov, DESY 95-029, hep-ph/9502308.

[6] C. Corianò, A.R. White, ANL-HEP-PR-95-19/UF-IFT-HEP-95-21, hep-ph/9510329.

[7] C. Corianò, A.R. White, Proceedings of the XXIV International Symposium on Multiparticle Dynamics, Vietri sul Mare, Italy 1994.

[8] V.N. Gribov, I.Ya. Pomeranchuk, K.A. Ter-Martirosyan, *Phys. Rev.* **139B**, 184 (1965).

[9] A.R. White, *Int. J. Mod. Phys.* **A6**, 1859 (1990).

[10] H.P. Stapp, A.R. White, *Phys. Rev.* **D26**, 2145 (1982).

[11] H.P. Stapp, in *Structural Analysis of Collision Amplitudes*, Proceedings of the Les Houches Institute, eds. R. Balian, D. Iagolnitzer, North-Holland 1976.

[12] A.R. White, *Phys. Lett.* **B334**, 87 (1994).

[13] G. 't Hooft, *Nucl. Phys.* **B33**, 173 (1971).

[14] A.R. White, *Int. J. Mod. Phys.* **A8**, 4755 (1993).

[15] R. Kirschner, LEIPZIG-18-1995, hep-ph/9505421.
[16] C. Corianò, A.R. White *Phys. Rev. Lett.* **74**, 4980 (1995); *Nucl. Phys.* **B451**, 231 (1995).
[17] J. Bartels, M. Wüsthoff, *Z. Phys.* **C66**, 157 (1995).
[18] C. Corianò, R.R. Parwani, A.R. White, ANL-HEP-PR-95-53/IFTIP-BBSR-95-80/UF-IFT-HEP-95-20.
[19] R. Kirschner, *Z. Phys.* **C65**, 505 (1995); L.N. Lipatov, *Phys. Lett.* **B251**, 284 (1990).
[20] J. Bartels, L.N. Lipatov, M. Wüsthoff, hep-ph/9509303.

t-CHANNEL UNITARITY CONSTRUCTION OF SMALL-x KERNELS*

C. CORIANÒ[a,b] AND A.R. WHITE[a]

[a]High Energy Physics Division
Argonne National Laboratory
9700 South Cass, Il 60439, USA
[b]Institute for Fundamental Theory
Department of Physics, University of Florida
Gainesville, FL 32611, USA

(Received November 3, 1995)

We present the BFKL equation as a reggeon Bethe–Salpeter equation and discuss the use of reggeon diagrams to obtain 2-2 and 2-4 reggeon interactions at $O(g^4)$. We then outline the dispersion theory basis of multiparticle j-plane analysis and describe how a gauge theory can be studied by combining Ward identity constraints with the group structure of reggeon interactions. The derivation of gluon reggeization, the $O(g^2)$ BFKL kernel, and $O(g^4)$ corrections, is described within this formalism. We give an explicit expression for the $O(g^4)$ forward "parton" kernel in terms of logarithms and evaluate the eigenvalues. A separately infra-red finite component with a holomorphically factorizable spectrum is shown to be present and conjectured to be a new leading-order partial-wave amplitude. A comparison is made with Kirschner's discussion of $O(g^4)$ contributions from the multi-Regge effective action.

PACS numbers: 11.55.Jy, 12.38.Lg

1. Introduction

In the leading-log approximation, the small-x behavior of parton distributions in QCD is derived from the BFKL evolution equation [1]. It is well-known that the BFKL kernel is (and was derived as) a 2-2 reggeon interaction — with the reggeon being a reggeized gluon. For general t $(= -q^2)$

* Presented by Alan R. White at the XXXV Cracow School of Theoretical Physics, Zakopane, Poland, June 4–14, 1995.